



Distinct ecotypes within a natural haloarchaeal population enable adaptation to changing environmental conditions without causing population sweeps

Tomeu Viver¹ · Roth E. Conrad² · Luis H. Orellana³ · Mercedes Urdiain¹ · José E. González-Pastor⁴ · Janet K. Hatt² · Rudolf Amann³ · Josefa Antón⁵ · Konstantinos T. Konstantinidis¹ · Ramon Rosselló-Móra¹

Received: 17 July 2020 / Revised: 26 October 2020 / Accepted: 11 November 2020 / Published online: 20 December 2020

© The Author(s), under exclusive licence to International Society for Microbial Ecology 2020

Abstract

Microbial communities thriving in hypersaline brines of solar salterns are highly resistant and resilient to environmental changes, and salinity is a major factor that deterministically influences community structure. Here, we demonstrate that this resilience occurs even after rapid osmotic shocks caused by a threefold change in salinity (a reduction from 34 to 12% salts) leading to massive amounts of archaeal cell lysis. Specifically, our temporal metagenomic datasets identified two co-occurring ecotypes within the most dominant archaeal population of the brines *Haloquadratum walsbyi* that exhibited different salt concentration preferences. The dominant ecotype was generally more abundant and occurred in high-salt conditions (34%); the low abundance ecotype always co-occurred but was enriched at salinities around 20% or lower and carried unique gene content related to solute transport and gene regulation. Despite their apparent distinct ecological preferences, the ecotypes did not outcompete each other presumably due to weak functional differentiation between them. Further, the osmotic shock selected for a temporal increase in taxonomic and functional diversity at both the *Hqr. walsbyi* population and whole-community levels supporting the specialization-disturbance hypothesis, that is, the expectation that disturbance favors generalists. Altogether, our results provide new insights into how intraspecies diversity is maintained in light of substantial gene-content differences and major environmental perturbations.

Supplementary information The online version of this article (<https://doi.org/10.1038/s41396-020-00842-5>) contains supplementary material, which is available to authorized users.

✉ Konstantinos T. Konstantinidis
kostas@ce.gatech.edu

✉ Ramon Rosselló-Móra
ramon@imedea.uib-csic.es

¹ Marine Microbiology Group, Department of Animal and Microbial Biodiversity, Mediterranean Institute for Advanced Studies (IMEDEA, CSIC-UIB), Esporles, Spain

² School of Civil and Environmental Engineering, Georgia Institute of Technology, Atlanta, GA, USA

³ Department of Molecular Ecology, Max-Planck-Institut für Marine Mikrobiologie, Bremen D-28359, Germany

⁴ Laboratory of Molecular Adaptation, Department of Molecular Evolution, Centro de Astrobiología, Consejo Superior de Investigaciones Científicas—Instituto Nacional de Técnica Aeroespacial, Madrid, Spain

⁵ Department of Physiology, Genetics and Microbiology, University of Alicante, Alicante, Spain

Introduction

Prokaryotic species are very diverse, e.g., some of them harbor more unique genes than the human genome [1, 2], while the number of distinct species on Earth has been estimated between several millions to a trillion [3]. Understanding the mechanisms generating and/or maintaining this biodiversity is one of the important challenges in microbial ecology. Several theories have recently been advanced to explain these diversity patterns. Among them, the ecological species concept suggests that the gene-content diversity within (or between) species offers strong competitive advantages, which often lead to diversity purging (loss) and speciation when the right conditions exist [4–6]. On the other hand, it's argued that most of the gene-content diversity within species is neutral (meaning functionally redundant or not important) or ephemeral, and thus diversity within species is maintained due to lack of competitive advantage, especially when conditions remain relatively stable [7–10]. In order to test these hypotheses, it is essential to quantify how diversity is

affected during periods of environmental transition or disturbance.

In plant and animal communities, generalist populations better withstand disturbances, whereas specialist populations are favored in stable environments. This is because most specialist taxa are adapted to relatively narrow niches in their natural ecosystem, and thus they are selected against when communities experience a severe disturbance, the so-called specialization-disturbance hypothesis [11]. Although some previous studies applied ecological theory to describe the response and recovery of community dynamics to disturbance [12, 13], the relationship of disturbance and specialization remains largely unexplored in microbial communities. Specifically, disturbed communities are often observed to encompass reduced taxonomic and/or phylogenetic diversity compared to undisturbed controls, but whether this pattern, which also translates to reduced functional diversity, remains largely unknown. We have recently shown that reduced taxonomic diversity, which coupled to increased functional diversity, characterizes the response of sedimentary microbial communities from Pensacola Beach (Florida, USA) to the Deepwater Horizon crude oil spill, i.e., the specialization-disturbance hypothesis applies in this case [14]. However, crude oil is a highly complex mixture of hydrocarbons, which could favor generalists (e.g., increased gene functional diversity) as opposed to specialists. Thus, whether other types of disturbances, which also elicit similar diversity patterns, remain to be tested. Moreover, it is important to test whether the same principle applies to the diversity patterns within a species or a population; that is, disturbance favors increased functional diversity within the species by mobilizing a larger fraction of the intraspecies gene content from its own rare biosphere compared to stable conditions.

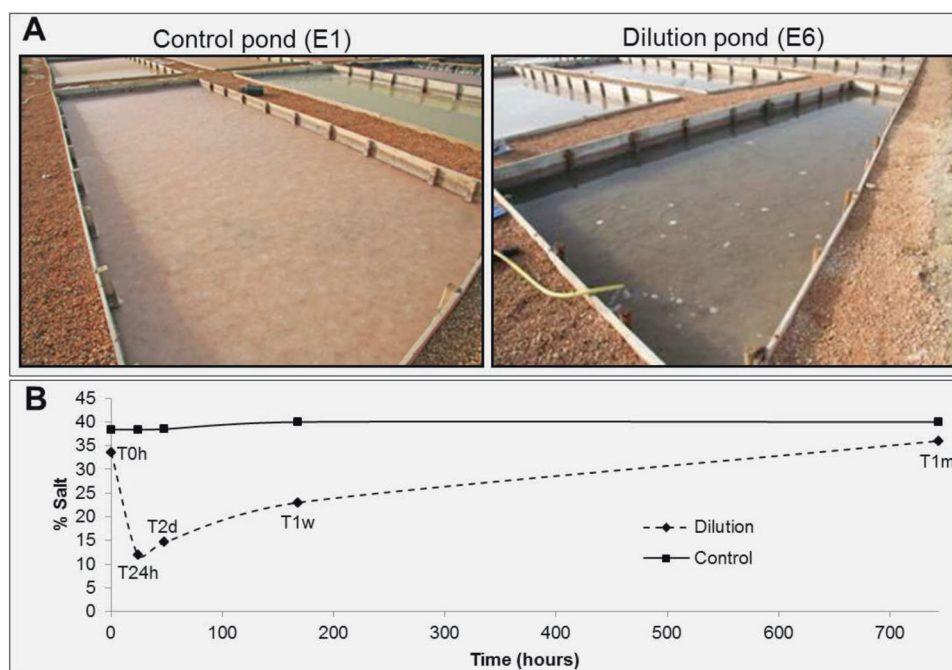
To test these hypotheses, it is also important to study the populations in situ, where the corresponding genes that underlie the mechanisms and/or speciation events can be better elucidated in response to perturbations or natural stimuli compared to the (typically) artificial conditions under laboratory settings. We have recently demonstrated that crystallizer ponds of solar salterns are excellent semi-natural systems at the mesocosm scale for use in testing ecological theories on resilience and resistance [1], and demonstrated that microbial communities highly resistant and resilient to change driven by irradiation and salinity deterministically establish in these ponds. An additional advantage of the solar salterns is their relatively low microbial diversity that appears to be at equilibrium, meaning that the less-adapted species have been out-competed [15]. These communities are generally dominated by three major lineages, i.e., *Halobacteriaceae*, *Nanoarchaeota*, and *Salinibacteraceae* with relatively low representation of distinct genera and species within each

lineage [16–19]. However, it has been shown by cultivation [20, 21] and molecular culture-independent methods [22] that the low species diversity is in contrast to high intraspecies strain diversity, at least for the two most abundant species thriving in the saltern environments, i.e., *Salinibacter ruber* and *Haloquadratum walsbyi* (*Hqr. walsbyi*). Whether this large intraspecific diversity is important for the success of the species in their changing environment (e.g., cycles of low and high salinity) or is mostly neutral (meaning ecologically redundant or not important) remains speculative [23].

Our specific model system, the solar salterns of Es Trenc, located in the south of Mallorca island (Spain), is a semi-artificial human-controlled environment fed with seawater (3.5% salts, mostly NaCl) and is structured as interconnected evaporation ponds with increasing salinities to reach salt saturation (>34% salts) in the crystallizers where salt precipitates (Fig. 1A). The semi-industrial production of salt is carried out on a spring–summer seasonal basis (early May to late September) and saturated brines are regularly refilled from the evaporating ponds to maintain volume and saturation conditions that are appropriate for salt precipitation. Once the harvest finishes at the end of summer and the heavy rains start that are typical of this western Mediterranean region [24], the ponds are no longer used until the following spring. Therefore, brine microbial communities are exposed to strong seasonal environmental changes (rainfall, temperature, irradiation, etc.), which are dynamic throughout the year [18]. Nonetheless, the microbial communities of these saltern systems are resilient to dilution and other stresses as evidenced by the fact that the community composition has remained similar during the 20 years that the Es Trenc brines have been studied [1, 17, 19, 20]. This stability indicates that these highly adapted assemblages have developed intrinsic strategies to maintain their diversity throughout the year in this dramatically fluctuating system.

To test the prevailing theories mentioned above, we employed metagenomic sequencing of temporal samples from the Es Trenc brines and comparative analysis of metagenome assembled genomes (MAGs) during a major salinity transition. We focused on the abundant archaeon of the salterns, *Hqr. walsbyi*, that has been shown to be more sensitive to dramatic changes [25]. In particular, we manipulated the salt concentration in one of the ponds by a sudden 2.8-fold dilution of the brine with the addition of freshwater (a reduction from 34 to 12% salts) simulating a heavy autumn rainfall event. We then assessed the effects of this event on the whole-community as well as the individual *Hqr. walsbyi* population diversity levels based on temporal samples collected over a month when salt saturation re-established due to natural evaporation. We evaluated which members of the community appeared to be more sensitive

Fig. 1 The experimental setup of the study. **A** Control pond E1 (left) is salt-saturated and therefore salt crystals are observed at the sediment interface; dilution pond E6 (right) have brines below the salt-saturation threshold, and therefore no salt precipitates form. **B** Salinity shifts throughout the experiment. Ponds were sampled at time zero (T0h), 1 day (T1), 2 days (T2), 1 week (T7), and 1 month (T31). After dilution, the E6 pond was not refilled during the experimental period.



and responsive to the dilution, what the community diversity patterns were post-dilution as salinity increased, and the genetic differences and dynamics at the ecotype level of the *Hqr. walsbyi* population. Here, we refer to “ecotype” with its original definition used to describe genetically determined differences between populations within a species that reflect local matches between the organisms and their environments, or different genotypes within a species having different fundamental niches [26].

Materials and methods

Experimental mesocosm description

Six adjacent crystallizer ponds, each of about 15 m³ in volume, were used in the year 2012 to observe the effect of different environmental pressures on the hyperhalophilic microbial communities. The ponds subjected to different light intensities were described elsewhere [1]; here, we focus primarily on the pond subjected to a dilution treatment and the control ponds. All ponds had been recently constructed and were used to concentrate salt for the first time. The same pre-concentrated seawater of the source concentrating pond was always used to fill and refill the experimental ponds in the 3 months prior to the experiment. To reach the salt saturation, crystallizers were refilled weekly to increase the concentration of salts from 17.2% that was the brine salt content of the inlet source in May to saturation, or near saturation (33.6–38.4%), in early August (Table S1). Pond E1, with saturating salt conditions (38.4%)

in early August, was used as a control for all experiments [1] and just experienced the natural environmental changes during the experiment. On the other hand, the main experiment pond, Pond E6, which was diluted as described below, was let to reach only near saturation conditions (i.e., 33.6% of salts) 2 weeks prior the experimental treatment (dilution) as opposed to salt-saturated conditions in order to minimize the effort required to dilute a salt-saturated pond with precipitated crystals. On the day the experiment started (early August), Pond E6 was filled with fresh groundwater (from an on-site groundwater well) using continuous flow and mixing to avoid stratification and reducing the salinity from 33.6–12% within 4 h (Table S1). Subsequently, the Pond E1 (control) and E6 (dilution treatment) were sampled for 1 month with no refilling; salt-saturation conditions re-established in Pond E6 after 1 month of sampling, hence no further sampling was performed after that point (Fig. 1B).

Metagenomics analysis

The detailed methodology employed here has been published previously [1]. Briefly, metagenomic coverage was predicted using Nonpareil v2.4 software [27]. MASH distance analyses [28] were visualized in an NMDS plot using the vegan library [29] in RStudio v3.2.2. 16S rRNA gene-encoding reads were extracted from metagenomes and clustered at 98.7% nucleotide identity using QIIME. The representative sequences from each operational taxonomic unit (OTU) were aligned using SINA [30] and added to the pre-calculated reference tree available in SILVA REF123 using the parsimony tool implemented in ARB [31]. The

tree topology was manually evaluated, and the OTUs affiliating with the same monophyletic branch with at least one almost complete representative sequence in the database were subsequently clustered into operational phylogenetic units (OPUs) as described previously [19].

Contigs with lengths over 1000 bp were binned into MAGs using MaxBin v2.1.1 [32] with default parameters. The average amino-acid identity (AAI) of each MAG against the NCBI isolate genome database was calculated using the Microbial Genomes Atlas (MiGA [33]). MAGs obtained from the control experiment [1] were labeled with a C (C-MAGs), and those obtained from the dilution pond with a D (D-MAGs; Tables 1 and S2). The abundance of MAGs in each metagenome was calculated by mapping the reads using BLASTn [34] and selecting reads with $\geq 95\%$ identity and alignment length $\geq 70\%$ because this level of identity represented the level of sequence diversity observed within the natural *Hqr. walsbyi* population. The number of mapped reads was divided by the total number of reads in each metagenome to provide the relative abundance of the MAG (% of total) or divided by the size (bp) of the total length of the MAG to provide the X coverage value (or sequencing depth).

Hqr. walsbyi MAGs were recovered from individual metagenomic datasets (no co-assembly was performed). Potential contamination of MAGs was removed following the tutorial available by Anvio's tools v5.5 [35]. Genes were predicted using Prodigal v2.6.3 [36]. Predicted proteins were annotated against the TrEMBL database [37] using blastp searches and selecting the best matches with sequence similarity $>50\%$ and over 50% of the query sequence length. Core and pangenome analysis was performed using all-versus-all BLAST with all MAGs. Recruitment plots for MAG contigs and genes and the average nucleotide identity of mapped reads values were calculated using the "enveomics.R" package v1.5 [38]. To calculate the abundance and gene-content diversity, read mapping against MAGs was performed by competitive best-match searches selecting those reads with sequence identity $>95\%$, which represents the most common threshold for species distinction based on sequence data [39, 40] and also accounts for genes that may evolve faster than the available *Hqr. Walsbyi* genome. The resulting read sequence depth data across the genome were averaged after the upper and lower 10% of outliers were removed providing the truncated average depth (or TAD80). To calculate the difference in abundance between different ecotypes and for a confident assignment, the analysis only took into account the reads that matched at 100% identity in one MAG and $<100\%$ in the rest. TAD80 values were normalized for dataset and genome size (when MAG completeness was not close to 100%) in order to provide relative abundance of the total estimates.

DAPI and CARD-FISH analysis

All samples were immediately fixed with formaldehyde and processed for the fluorescence microscope counts as previously reported [41]. Total quantification of microorganisms was performed by DAPI, and the bacterial and archaeal fractions were separately assessed by applying CARD-FISH with domain-specific probes as detailed in Viver et al. [41].

Results

Whole microbial community shifts

The pond (E6) used to perform the osmotic shock effect (i.e., dilution) contained brines at a concentration of 33.6% salts just below the saturation point (NaCl saturation occurs at salinities reaching 36% at 25°C [42]; Table S1). On the other hand, the E1 was saturated (38.4%) with visually obvious salt precipitates (Fig. 1) and was used as a control. Despite the difference in salt saturation, both control and E6 showed very similar total cell counts (DAPI; $\sim 4 \times 10^7 \pm 2.4$ cells/ml) and relative abundances of the bacterial and archaeal domains ($\sim 21\%$ and 79%, respectively; Table S3A). However, differences in relative abundance and richness of bacterial OPU (Kolmogorov–Smirnov test p values >0.05 ; Table S4) were observed with the unsaturated E6 having higher values (Table S5). In both ponds, the most abundant archaeal OPU affiliated with *Haloquadratum* sp. (8.83% for E1 and 3.73% for E6; Fig. S1), and the most abundant bacterial OPU with *Salinibacter* sp. (20.3% for E1 and 17.4% for E6; Fig. S1). E6 also showed a substantial presence of *Spiribacter* spp. (7.9%) and some uncultured *Rhodobacteraceae* (3.6%). Relative abundance based on read recruitment of the C-MAGs (Table 1 and Fig. 2) mirrored the OPU relative abundance results, with *Haloquadratum* sp. and *Salinibacter* sp. MAGs exhibiting higher abundances in the control. In contrast, the halo-bacterial MAGs C6 (0.22% in E6 and 0.16% in E1), C11 (0.52% in E6 and 0.049% in E1), C16 (1.99% in E6 and 0.84% in E1), and C30 (1.01% in E6 and 0.082% in E1) were higher in E6.

The fast dilution of E6 from 33.6 to 12% salts within 4 h (2.8-fold salinity drop with a rate of 5.4% salinity/hour) produced a dramatic change in the cell numbers with a decrease from $4.4 \pm 2.58 \times 10^7$ cells/ml to $6.93 \pm 0.15 \times 10^6$ cells/ml (Table S3A). We did not expect any influence from the cells present in the added groundwater because the concentration of these cells should be two to six orders of magnitude lower than the cells of the brines, and groundwater cells should not be adapted to high-salt concentrations; hence, these organisms would die out quickly when

Table 1 Statistics of MAGs recovered from dilution (D-MAGs) and control metagenomes (C-MAGs).

| MAGs | Contigs | Bases (Mb) | % GC | Compl. (%) | Cont. (%) | Taxon | Lower rank classification |
|-------------------------------|---------|------------|-------|------------|-----------|-----------------------------|---------------------------|
| Dilution pond (D-MAGs) | | | | | | | |
| Archaea | | | | | | | |
| D2 | 341 | 2.96 | 47.60 | 100 | 0 | <i>Hqr. walsbyi</i> | Species |
| D4 | 572 | 1.85 | 68.60 | 69.2 | 0 | <i>Halorubrum</i> sp. | Genus |
| D5 | 128 | 2.01 | 66.39 | 53.8 | 0 | <i>Natronomonas</i> sp. | Genus |
| D8 | 126 | 1.09 | 67.10 | 69.2 | 0 | <i>Haloferacaceae</i> sp. | Family |
| D11 | 137 | 0.59 | 66.30 | 50.0 | 0 | <i>Natronomonas</i> sp. | Genus |
| D14 | 520 | 1.55 | 66.64 | 53.8 | 11.5 | <i>Halorubrum</i> sp. | Genus |
| D15 | 128 | 0.42 | 66.70 | 46.2 | 0 | <i>Halobacteriaceae</i> sp. | Family |
| D16 | 591 | 1.63 | 70.10 | 34.6 | 7.7 | <i>Haloferacaceae</i> sp. | Family |
| D18 | 760 | 2.04 | 70.10 | 61.5 | 11.5 | <i>Halorubrum</i> sp. | Genus |
| D26 | 305 | 1.18 | 68.80 | 53.8 | 0 | <i>Haloferacales</i> sp. | Order |
| Bacteria | | | | | | | |
| D1 | 575 | 3.27 | 66.20 | 85.6 | 7.2 | <i>Salinibacter</i> sp. | Genus |
| D3 | 409 | 4.24 | 66.50 | 95.5 | 13.5 | <i>Rhodothermaceae</i> sp. | Family |
| D6 | 676 | 4.29 | 66.70 | 86.3 | 22.5 | <i>Salinibacter</i> sp. | Genus |
| D9 | 295 | 2.52 | 53.20 | 92.8 | 4.5 | <i>Bacteroidetes</i> sp. | Phylum |
| D12 | 578 | 1.86 | 60.36 | 50 | 13.7 | <i>Rhodothermaceae</i> sp. | Family |
| D13 | 2097 | 4.89 | 69.38 | 63.7 | 13.7 | <i>Rhodovibrio</i> sp. | Genus |
| D19 | 1868 | 3.63 | 57.01 | 71.2 | 10.8 | <i>Marinobacter</i> sp. | Genus |
| D22 | 1053 | 2.51 | 65.26 | 87.3 | 22.5 | <i>Spiribacter</i> sp. | Genus |
| D23 | 1155 | 2.07 | 34.99 | 43.2 | 5.4 | <i>Flavobacteriia</i> sp. | Class |
| D24 | 662 | 3.13 | 41.90 | 89.2 | 7.2 | <i>Flavobacteriia</i> sp. | Class |
| D25 | 1551 | 2.63 | 47.20 | 55.9 | 13.5 | <i>Bacteroidetes</i> sp. | Phylum |
| <i>Hqr. walsbyi</i> | | | | | | | |
| D1T0 | 258 | 3.06 | 47.53 | 100 | 0 | <i>Hqr. walsbyi</i> | Species |
| D2T1 | 371 | 3.61 | 47.81 | 100 | 0 | <i>Hqr. walsbyi</i> | Species |
| D2T2 | 176 | 2.97 | 47.52 | 100 | 0 | <i>Hqr. walsbyi</i> | Species |
| D2T7 | 840 | 2.43 | 46.82 | 47.8 | 0 | <i>Hqr. walsbyi</i> | Species |
| D2T31 | 479 | 2.73 | 47.52 | 95.7 | 0 | <i>Hqr. walsbyi</i> | Species |
| Control pond (C-MAGs) | | | | | | | |
| Archaea | | | | | | | |
| C1 | 542 | 1.49 | 47.94 | 57.7 | 0.0 | <i>Hqr. walsbyi</i> | Species |
| C3 | 1111 | 2.04 | 62.27 | 26.9 | 0.0 | <i>Halobacteriales</i> sp. | Order |
| C4 | 502 | 2.31 | 67.36 | 69.28 | 7.7 | <i>Halorubraceae</i> sp. | Falimy |
| C5 | 765 | 3.29 | 63.72 | 91.59 | 13.6 | <i>Haloarculaceae</i> sp. | Family |
| C6 | 286 | 2.71 | 50.83 | 88.88 | 2.1 | <i>Haloferacales</i> sp. | Order |
| C8 | 647 | 2.32 | 64.51 | 53.99 | 11.5 | <i>Haloferacales</i> sp. | Order |
| C11 | 1075 | 2.86 | 69.79 | 87.00 | 4.3 | <i>Halobacteriaceae</i> sp. | Family |
| C14 | 487 | 1.26 | 69.79 | 52.93 | 8.8 | <i>Halobacteriaceae</i> sp. | Family |
| C16 | 548 | 2.74 | 69.79 | 46.20 | 3.8 | <i>Halorubraceae</i> sp. | Falimy |
| C21 | 898 | 2.24 | 61.74 | 43.50 | 8.7 | <i>Halobacteriaceae</i> sp. | Family |
| C22 | 1113 | 2.11 | 66.91 | 34.60 | 0.0 | <i>Halorubraceae</i> sp. | Family |
| C28 | 437 | 0.83 | 68.51 | 28.62 | 3.8 | <i>Halobacteriaceae</i> sp. | Family |
| C29 | 246 | 0.64 | 65.79 | 18.48 | 0.0 | <i>Halorubraceae</i> sp. | Family |
| C30 | 662 | 0.87 | 64.67 | 23.49 | 3.5 | <i>Halobacteria</i> sp. | Class |
| C31 | 389 | 0.92 | 68.93 | 29.91 | 1.9 | <i>Haloferacaceae</i> sp. | Family |
| C32 | 195 | 1.08 | 43.49 | 91.30 | 13 | <i>Nanohaloarchaea</i> sp. | Class |
| Bact | | | | | | | |
| C2 | 874 | 2.13 | 64.86 | 88.88 | 2.1 | <i>Salinibacter</i> sp. | Family |
| C20 | 1149 | 2.25 | 63.52 | 59.17 | 25.7 | <i>Rhodothermaceae</i> sp. | Family |

The complete information of the MAGs is reported in Tables S2 and S9. Note that C-MAGs have been described previously [1].

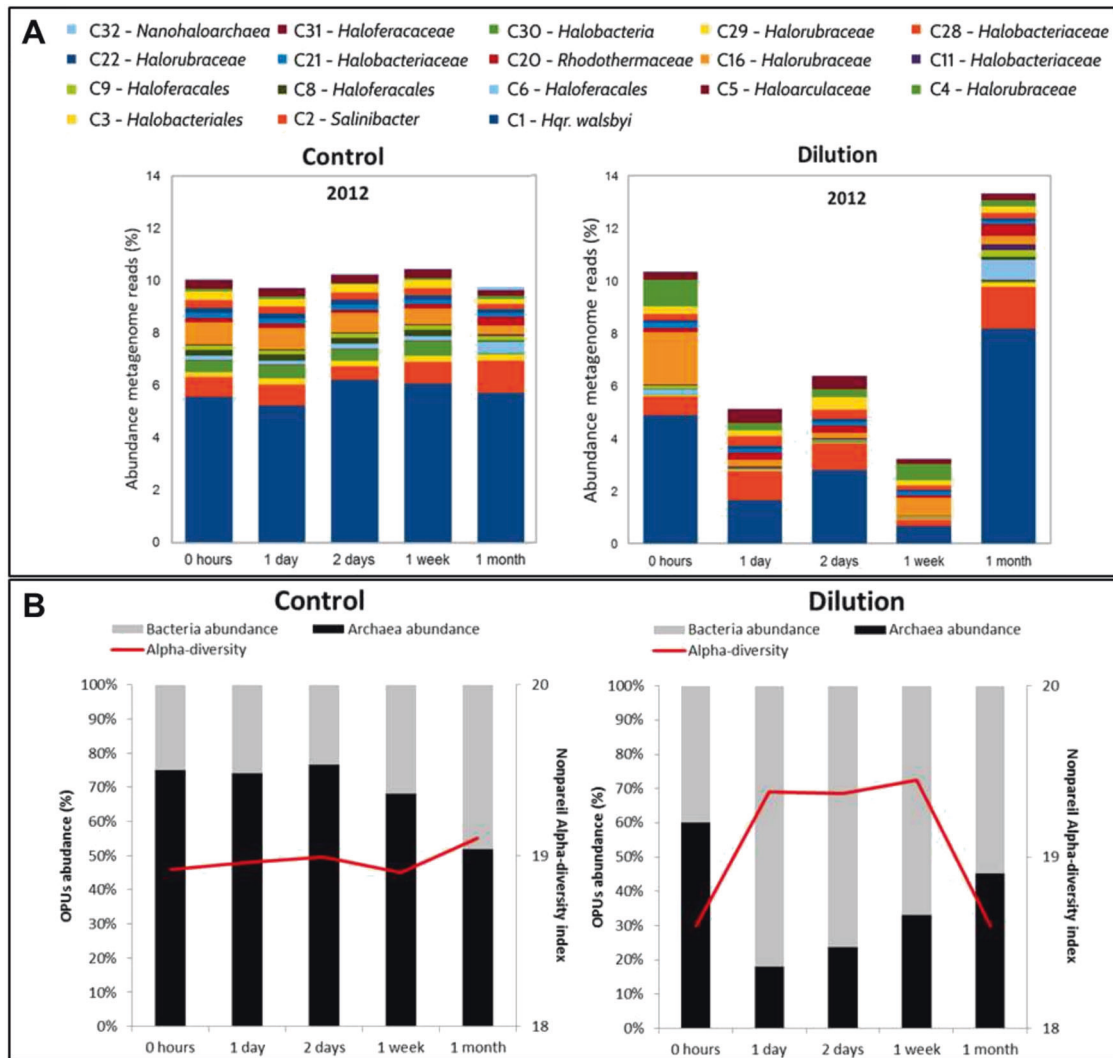


Fig. 2 Taxonomic shifts during the dilution experiment. **A** Shifts in abundance of the C-MAGs. **B** Dynamics of the archaeal vs. bacterial fraction of the communities based on OPUs (bars; primary y axis), and alpha diversity based on Nonpareil (red line; secondary y axis).

such conditions prevail due to evaporation [43]. This 6.7-fold concentration decrease (Table S3B) contrasted with the expected 2.8-fold change due to dilution alone. The archaeal cells were most sensitive since they decreased 17.5-fold in abundance, while their bacterial counterparts just experienced a 2.8-fold decline (Table S3B). Accordingly, all halobacterial OPU's decreased in their relative abundances (Fig. S1 and Table S5) leading to significant differences in taxonomic structure pre- and post-osmotic shock (p value < 0.05 on Kolmogorov–Smirnov test; Table S4). The sequence diversity as measured by Nonpareil curves increased from 18.6 to 19.38 (Fig. 2b and Table S6; note that Nonpareil diversity is reported in \log_{10} units), and Chao-1 values based on OPU's increased from 129 OPU's to 290 OPU's (Table S5) after the osmotic shock indicating increased alpha diversity. In both cases, the bacterial fraction was mainly responsible for the

differences. Interestingly, the increase in taxonomic diversity was accompanied by an increase in functional gene diversity as evidenced—for instance—by the fact that at least 50 additional subsystems were observed in the early metagenomes after the dilution event relative to the control or to the 1-month metagenomes (Fig. 3). The average genome size of the microbial community was also significantly higher in these early metagenomes, consistently indicating that generalist taxa were favored by the osmotic shock.

Subsequently, the brine experienced a natural evaporation (by sunlight) raising the salinity from 12 to 23% salts within just 1 week (Fig. 1), and to saturation (36% salts) after 1 month with visible salt precipitates on the sediment surface. An intermediate increase in diversity occurred during the first week (Fig. 2b) and gradually reduced toward the end of the experiment as evidenced by (i) an increase in

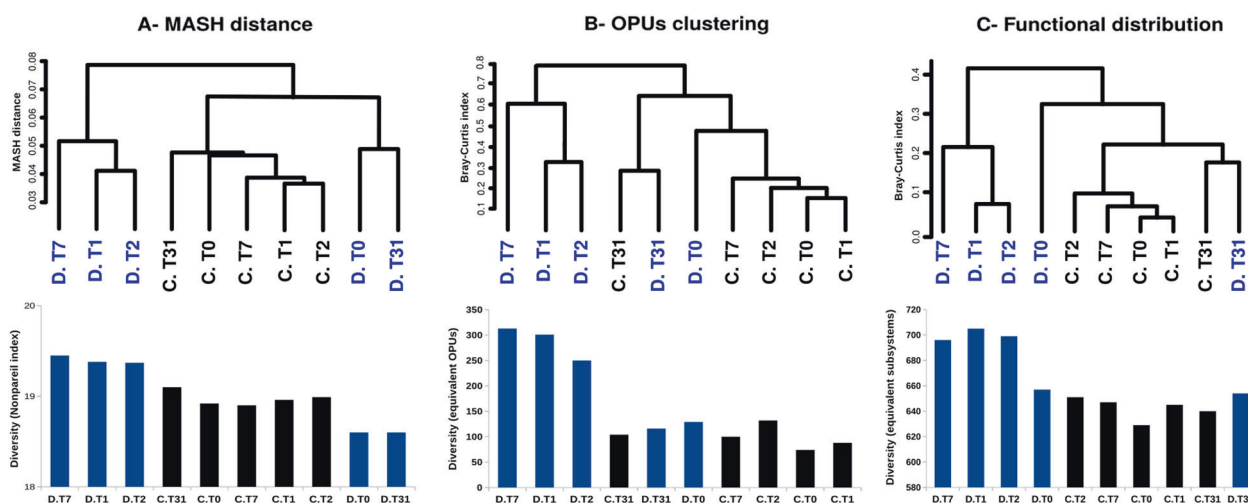


Fig. 3 Similarity among the metagenomes determined in this study. Clustering of all metagenomes based on: **A** whole metagenome MASH distance, **B** Jaccard distance based on OPU, **C** the abundance

the percentage of reads mapping to contigs longer than 500 bps assembled from the corresponding metagenomes (~45% in diluted early metagenomes vs. ~65% in high salinity metagenomes; Supplementary Spreadsheet Table T1), (ii) a tenfold decrease in the alpha diversity estimated by Nonpareil (~19.4 in diluted samples and 18.6 in high salinity; Fig. 2b and Table S6), and (iii) a gradual decrease of Shannon indices based on OPU (Table S5). All cluster analyses performed on the species (OPUs), genes, or short reads consistently revealed two groups (Fig. 3): a low salinity group composed of E6 1 day (T1), 2 days (T2), and 1 week (T7) metagenomes, and a high salinity group composed of E6 T0 and 1 month (T31) and all of the control E1 metagenomes. Accordingly, the MinHash distances between the E1 (control) and E6 initial (e.g., time 1 day or T1) metagenomes showed that the two communities were different. The distances to the control pond increased after the osmotic shock to a maximum distance at the 1-week metagenome before finally decreasing to the lowest distance at the end of the experiment once saturation conditions were reached (Fig. 3A). Furthermore, despite clustering together, the three low salinity intermediate metagenomes (i.e., T1, T2, and T7) were not identical according to the Kolmogorov–Smirnov test (Table S4) and showed the highest numbers of sample-unique OPU (Figs. 3 and S2).

MAG diversity and shifts

The metagenomes of the intermediate stages (T1, T2, and T7) of E6 yielded 21 D-MAGs (Table 1), ten affiliated with the class *Halobacteria* and eleven with different bacterial lineages. Among the archaeal D-MAGs, only one (D2 identified as *Hqr. walsbyi*) was assignable to a known species with an AAI value of 98.79% (Sup. Table S2),

of SEED subsystems. Metagenomes of the control pond E1 are labeled in black and those of the dilution pond E6 in blue.

whereas five (D4, D5, D11, D14, and D18) exhibited AAI values between 70 and 90% indicating that the corresponding MAGs belong to known genera but unclassified species [44]. An additional four MAGs (D8, D15, D16, and D26) were very distantly related to classified taxa with AAI values <65% against all genomes and MAGs available in public repositories (according to MiGA [33]). Among the eleven bacterial D-MAGs assembled, four affiliated with the family *Salinibacteraceae*, two with AAI values <65% (D3 and D12), one with a 67.9% AAI (D1), and one true member of *Sal. ruber* with a 98.9% ANI, and 95.9% AAI (D6) with the genome of the type strain (Table S2). The D-MAGs D13 (*Rhodovibrio* sp.), D19 (*Marinobacter* sp.), and D22 (*Spiribacter* sp.) showed AAI values between 70 and 90% with the genomes of their respective type species, and finally, four D-MAGs affiliated with *Bacteroidetes* all had <65% AAI (D9, D23, D24, and D25) with the genomes of their closest relatives. It was remarkable that we recovered nearly identical MAGs (ANI values >98.9%) from different ponds including D2 and C1 (*Hqr. walsbyi*), D18 and C16 (*Halorubrum* sp.), and D1 and C2 (*Salinibacter* sp.).

The relative abundances of the C- and D-MAGs based on read recruitment (Fig. 4) showed three main dynamics: (i) species that promptly decreased in abundance after the osmotic shock presumably due to cell lysis (T1, T2, and T7), i.e., all archaeal C-MAGs, but their abundances largely recovered by 1 month (T31). (ii) Species resistant to the osmotic shock that showed a slightly increased abundance just after the stress (T1 and T2), but with an intermediate decline to finally recover in the long term, which included all MAGs identified as *Salinibacter* sp. and, (iii) species that increased in abundance immediately after the shock and throughout the intermediate stages when low salinities prevailed, i.e., the majority of D-MAGs (mostly

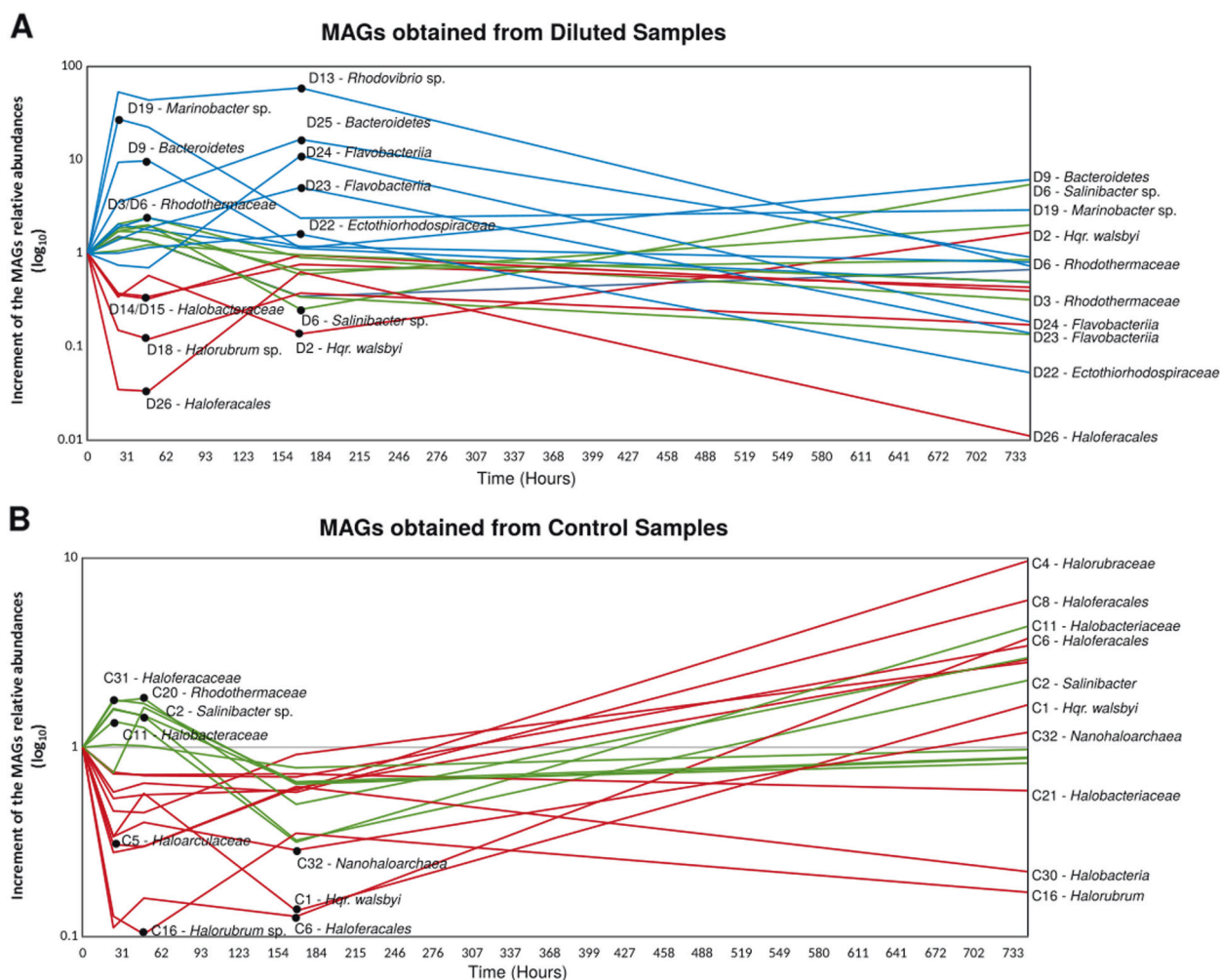


Fig. 4 Shifts in the abundances of the control and dilution MAGs during the sampling period. **A** D-MAGs and **B** C-MAGs. MAGs that decreased in abundance after the osmotic shock are shown in red while those that increased in abundance after osmotic shock but decreased

after 1 week of dilution are shown in green. MAGs that increased in abundance in the intermediate salinities (i.e., T1, T2, and T7 time points) are shown in blue for comparison.

bacterial), and especially *Rhodovibrio* sp. (OPU305 and MAG D13).

There were several relevant gene functions that changed more than twofold in abundance relative to the control (Tables S7 and S8). In the intermediate stages, we observed an increased number of subsystems related to the accumulation of organic compatible solutes such as sarcosine, ectoine, betaine, glycine; synthesis of osmoregulated periplasmic glucans, and Na^+/H^+ antiporters. We also detected an increased occurrence of genes related to biosynthesis and degradation of chlorophyll, photorespiration, and photosystem I and II genes in accordance with a higher occurrence of cyanobacterial OPUs (Table S8). Similarly, we detected an intermediate increase in the occurrence of genes related to the metabolism, breakdown, and mineralization of dimethyl sulfide and dimethyl sulfoniopropionate. On the other hand, the saturated or close to saturation samples showed increased subsystems associated with potassium

homeostasis (>33%; Table S8). In general, MAG-based patterns were consistent with the community-wide shifts mentioned above in that MAG diversity, genome size, and functional repertoire temporarily increased after the dilution event before decreasing when salt-saturation conditions re-established at 1 month post dilution.

Hqr. walsbyi ecotype shifts

The only taxon recovered as a single MAG in all the metagenomes was *Hqr. walsbyi*. MAGs D2T0, D2T1, D2T2, D2T7, and D2T31 were all obtained with high coverage (>6X to ~102X) in their respective metagenomes (Tables 1 and S9). All five MAGs had ANI values >98.5% compared to the genome of the type strain *Hqr. walsbyi* C23^T and >99.5% among themselves, but none were identical to each other (Table S10). Based on slightly different ANI values, and especially the number of shared

orthologous genes, we could identify two different MAG groups. One group was composed of four MAGs D2T0, D2T1, D2T2, and D2T31 (assigned as ecotype 1; Hwals1) that shared ANI > 99.73% and the highest amount of orthologous genes. A single MAG D2T7 (assigned as ecotype 2; Hwals2), recovered after 1 week, made up the other group and showed the largest differences compared to the remaining MAGs in terms of ANI (~99.65%; Table S10) and MAG-specific orthologous genes (911 genes; Fig. S3). As a MAG represents the average composite genome of the most abundant genotype(s) at the time of sampling, the ANI and gene-content differences observed between the two groups pointed to the existence of (at least) two different ecotypes, which was further supported by their different abundance patterns along the salinity transition. Both ecotypes always coexist as revealed by competitive blast and recruitment plots of their corresponding MAGs (Figs. 5 and S4). The ecotype Hwals1 was always the most

abundant throughout the experiment in both control and diluted ponds, while the ecotype Hwals2 was generally of lower abundance (in general, ~2.5-fold lower) except 1 week after dilution when the salinity was about 24% and Hwals2 became even more abundant than Hwals1. Both ecotypes suffered a strong decline after the osmotic shock (between three- to fivefold), but the dominant ecotype suffered a stronger decline than Hwals2 (Fig. 5). During the period of salinity increase from 12 to 23% (i.e., from day 1 to day 7), the dominant ecotype still experienced a continuous decline in abundance, whereas Hwals2's abundance remained relatively stable or increased. After 1 month, when salinity reached saturation, relative abundances recovered with the dominant ecotype becoming more abundant.

Notably, all read recruitments of each MAG against any of the metagenomes exhibited a bimodal gene coverage with about 10% of the genes with lower coverage as

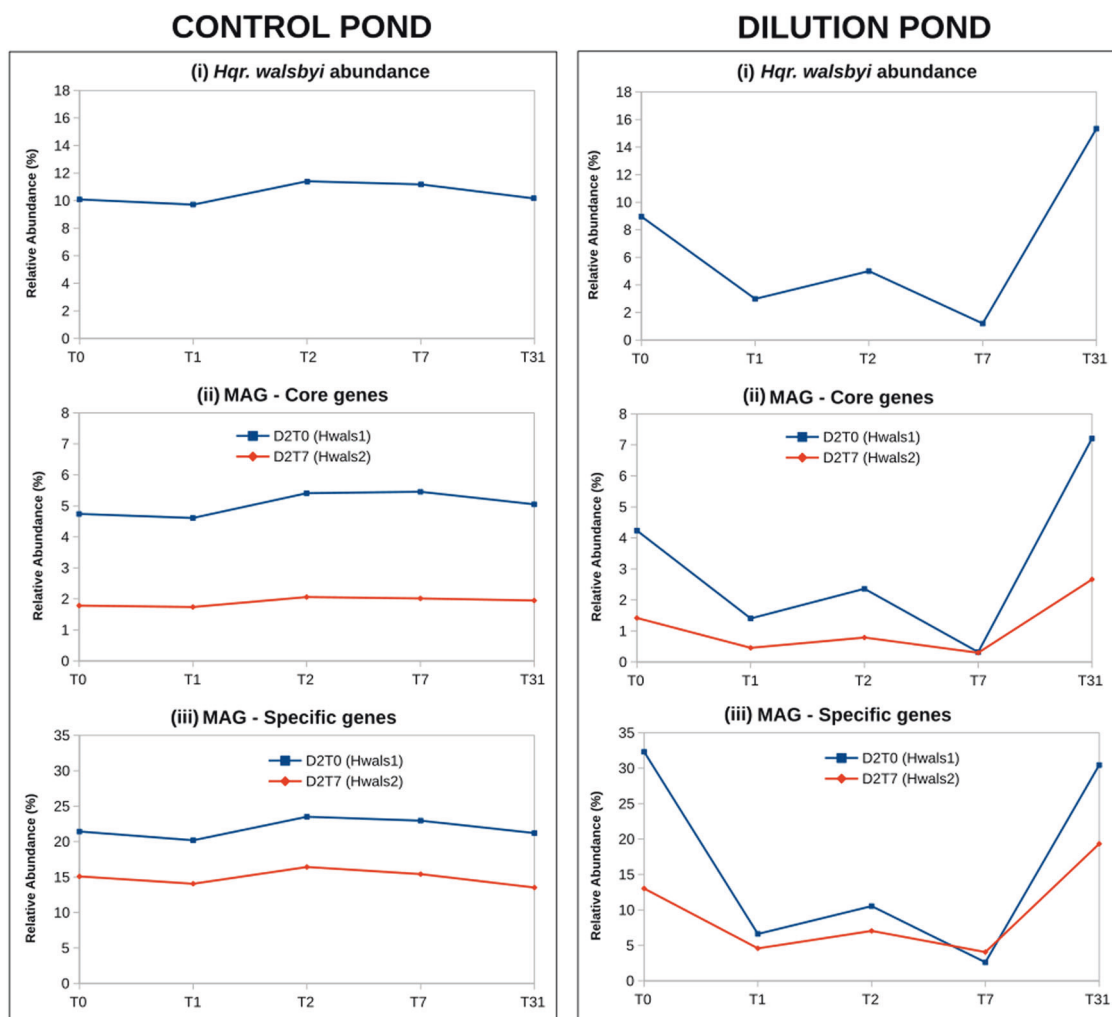


Fig. 5 Dynamics of the two *Haloquadratum walsbyi* ecotypes. Metagenomic relative abundance of reads from control (left column) and dilution pond (right column) mapping to (i) core MAG genes with

identity >98%, (ii) relative abundance based on competitive blast of reads mapping to core genes, and (iii) to MAG-specific genes.

assessed by TAD80 values (truncated average sequencing depth; Fig. S5). These gene coverage patterns further corroborated the existence of (at least) two ecotypes and the gene-content differences observed when comparing the MAG sequences to each other. In general, the set of genes that appeared specific to the most prevalent MAG group showed similar abundance to the core genes in T0, T1, T2, and T31 metagenomes but reduced coverage in the metagenome T7 (Figs. S5 and S6). Reciprocally, the Hwals-specific genes showed reduced occurrence in the other metagenomes except T7. These patterns indicated that the Hwals2-specific genes might be important for adaptation at low and intermediate salinities (Fig. 5). Consistent with this interpretation, the functional annotation of the Hwals2-specific genes revealed at least two genomic islands enriched in proteins for solute transport (e.g., an ABC-type transport system of amino acids and other small organic compounds), gene regulation and a glycosyltransferase, which altogether might play a role in osmoregulation, together with CRISPR-associated endonucleases, integrases, transposases, and hypothetical proteins (Fig. 6). The Hwals2 was also the only MAG containing the type-II secretion system to translocate proteins from the periplasm. Analogously, the Hwals1-specific genes included functions potentially involved in osmoregulation of (different) solutes, different transporter systems and ATP-binding proteins. Collectively, these results indicated that even though the osmotic shock negatively affected both *Hqr. walsbyi* ecotypes presumably due to cell lysis, Hwals2 recovered faster in the early stages after disruption, and the major ecotype needed a longer time and/or higher salinities for recovery. Most probably, Hwals2 represents a genotype adapted to lower salinity that is facilitated by its unique gene content, and the Hwals1 is the dominant genotype that is successful in the most extreme salt concentration.

Conspicuously, the four MAGs assigned to the dominant ecotype were not identical to each other but contained substantial gene-content difference and allelic variation in the shared genes (Figs. S7 and S8). Especially the intermediate stages represented by D2T1, D2T2 that harbored 745 and 788 divergent shared genes, respectively, were most divergent from D2T0 showing 99.8–98% nucleotide identity to their D2T0 homolog. Presumably these MAGs were the result of binning more diverse strains (genotypes) that became more abundant at the intermediate stages relative to the beginning or end of the experiment that was characterized by more stable conditions. Consistent with this interpretation, D2T0 and D2T31 were the most similar having the lowest amount of divergent genes. Therefore, it appears that the dilution disturbance selected (temporarily) for more diversity and more functions even within the *Hqr. walsbyi* population, consistent with the specialization-disturbance hypothesis.

Discussion

Here we challenged brine assemblages with a sudden dilution that simulated an autumn heavy rain, which could lead to community changes beyond the stability threshold. The nearly threefold dilution event promoted an uneven disturbance effect on the community. As previously observed [25], bacterial cells were much more resistant to the osmotic shock than their archaeal counterparts, presumably due to their stronger cell structure and the adaptation of their proteomes [45]. The archaeal cell lysis that resulted in a nearly sevenfold drop in abundance allowed a temporary increase of some members of the low abundance “rare” bacterial biosphere [46]. These bacteria were presumably resistant to osmotic shock, better adapted to lower salinity concentrations, and possibly profited—for instance—from the suddenly available growth substrates due to cell lysis. It may be that haloarchaea are adapted to a certain level of ionic stability so when unusual events such as heavy rains occur, their communities can be strongly devastated with irreversible shifts as previously hypothesized [47]. Despite the severe decline in one major microbial component, the nearly threefold dilution did not affect the community beyond the stability threshold nor its capacity to recover fully 1 month later when high-salt conditions were re-established due to evaporation. Therefore, it appears that the effect of the dilution shock was still within the environmental variation that the community could tolerate [15]. There must have been residual non-lysed cells perhaps consisting of better-adapted co-existing phylotypes [48] that presumably acted as a seed-bank [46], or there may be microniches of hypersaline brines that due to ineffective mixing (e.g., stratification due to different densities) acted as a microbial reservoir for the recolonization. Our findings also give a more optimistic view on the reported massive extinction in the Atacama Desert [47], as it might just take some time, in the case of the Atacama Desert even years [49], for the restoration of the salinity conditions and the reestablishment of the abundant members of the original communities. The salinity range variation observed here might be, if not the largest, one of the broader variations occurring in natural environments.

The salinity increases, in the short-term and after the shock, promoted community shifts compatible with expectation based on previous knowledge about what taxa are adapted to intermediate salinities (15–25%) with dominance of *Proteobacteria*, *Cyanobacteria*, *Bacteroidetes*, and to a minor extent *Halobacteria* [18, 50]. The punctuated increase of moderately halophilic organisms such as *Natronomonas* spp [51] was consistent with these interpretations, as were the enhanced occurrence of the compatible-solute gene-content repertoire observed in the intermediate-salinity metagenomes. These organisms tolerate high salt based on

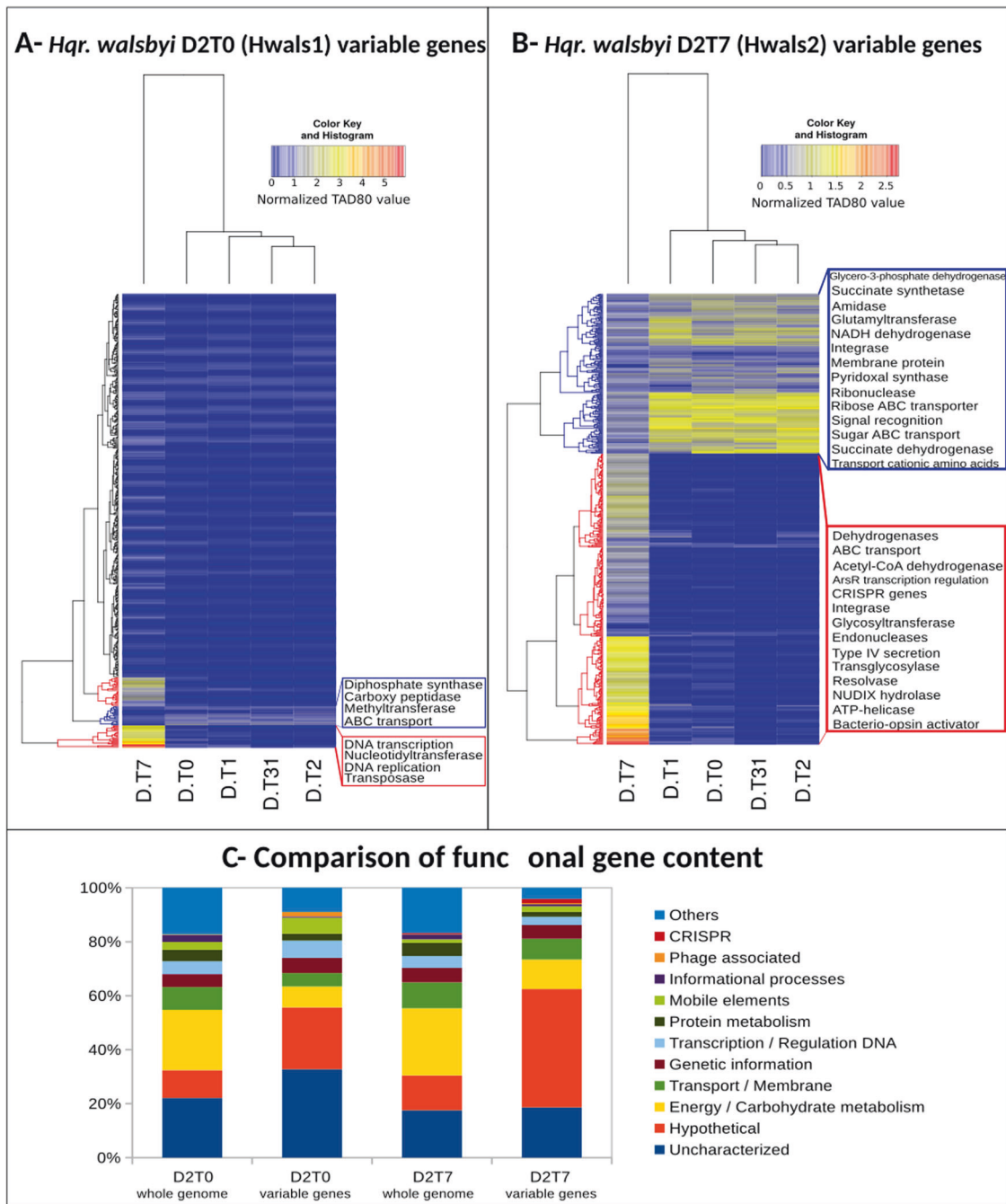


Fig. 6 *Hqr. walsbyi* D2T0 and D2T7 gene-content variability depending on normalized gene coverage (geneTAD80/avg. genome TAD80) and comparison of functional gene content between whole MAG genes and variable MAG genes. **A** Metagenome clustering based on normalized TAD80 values using the variable genes of the MAG D2T0. Gene clusters (vertical clustering) in red indicate genes with high coverage in sample T7 and in blue, genes with lower

coverage in the sample T7. Red and blue boxes indicate the gene function of the marked clusters. **B** Same representation as **A** but using variable genes of the MAG D2T7 as a reference. **C** Comparison of the functional gene content of MAG D2T0 and D2T7 and the functions encoded for the variable genes represented in **A** and **B**. Genes were annotated against TrEMBL databases. The numbers of genes were normalized to 100% to compare functional categories.

the acquisition and/or production of compatible organic solutes [45, 52] contrasting with extreme halophiles, which are characterized by built-in intracellular salt strategists, e.g., accumulation of KCl and the dominance of acidic proteins in the proteome [45].

In general, the saltern microbial communities changed both taxonomically and functionally after the dilution shock. The community shifts caused an increase in taxonomic diversity in early phases (intermediate salinities) with a significant recovery and reduction in taxonomic diversity

by 1 month when high-salt conditions re-established. This increase in taxonomic diversity was accompanied by an increase in functional diversity and larger genome sizes, in general (Fig. 3). Notably, a larger genome size and a greater number of functions were observed both at the whole-community and the individual *Hqr. walsbyi* population levels by our sequencing effort even when normalized to the metagenome with the lowest sequencing effort (Fig. S9). Therefore, our results are only partially consistent with the specialization-disturbance hypothesis [11] in that we observed a selection for generalist taxa shortly after the perturbation, but this was not accompanied by a reduction in taxonomic or phylogenetic diversity. These results contrasted with those of our previous study in which generalist taxa were selected for in coastal sedimentary communities perturbed by an oil spill with a concomitant reduction in taxonomic diversity apparently caused by oil toxicity and/or growth arrest due to limited hydrocarbon degradation capabilities of the typical oligotrophic taxa that are autochthonous to coastal sediments [14]. We had anticipated that carbon and energy sources would be affected much less by the dilution perturbation performed in the present study compared to the oil spill. Therefore, these findings revealed that different types of perturbations might elicit different responses to the corresponding microbial communities. Further, our results in terms of taxonomic diversity appear to be more compatible with the “intermediate disturbance hypothesis” [15], which predicts that intermediate (not extreme) environmental conditions maintain large diversity. Overall, our results provide evidence of complex successional patterns in the studied communities involving proliferation of rare members promoted by available organic material from cell lysis and intermediate salt conditions, and resulting in a general recovery of diversity, specialization, and halophilic groups a month after the disturbance.

Enabled by the high resolution provided by metagenome sequencing and genome binning, we were able to distinguish two different ecotypes of the dominant *Hqr. walsbyi* population. Although the ecotypes co-existed for the whole duration of our experiment, they showed distinct patterns in terms of preference for optimal salinity concentration and gene-content differences that most likely underlie their salinity preference. This genetic flexibility of *Hqr. walsbyi* is based on several genomic islands [22] that encode genes contributing to organismal fitness e.g., genes related to cell surface structures or S-layer proteins that may contribute to capsule formation [53]. Interestingly, while the abundance of the majority of ecotype-specific genes remained low as conditions changed (compared to shared genes), at least a handful of them were found to increase considerably in abundance in the metagenome from which the corresponding MAGs originated, e.g., MAG Hwals2-specific genes were more abundant in the 1-week metagenome, and that of the dominant ecotype were

more abundant in the other sampling dates. Notably, the predicted functions encoded by some of these genes were associated with environmental sensing, metabolite transport in/out of the cell, and gene regulation (Fig. 6). Collectively, these results further supported our hypothesis that the identified genes of MAG Hwals2 involved in regulation and transport are presumably important for cell osmoregulation under low- and intermediate-salinity conditions. It is also possible that additional functions important for salinity adaptation are hidden among the many hypothetical or unannotated proteins (~55% of the total) of the MAG Hwals2-specific genes [54]. The exact functions or substrate specificity of the identified genes remain unknown as bioinformatics analysis provides only general functional prediction. However, MAG-specific functions may facilitate the *Hqr. walsbyi* population in adapting to changes in salinity concentrations and are likely not neutral or ephemeral, but these findings await experimental testing.

An emerging question based on these findings is why the intrapopulation diversity was not purged (removed) when salinity conditions changed. That is, the ecotype (cells) that encodes the abovementioned genes should have outcompeted the other ecotype(s) of the population resulting in a more clonal population. However, relative abundance of ecotype-specific genes and competitive read mapping on shared (core) genes (Fig. 5) suggested that the ecotypes co-existed and intrapopulation diversity was maintained. Thus, we hypothesize that the ecological advantage of these genes is significant, but not strong enough to purge the intrapopulation diversity (or sweep through the population). Alternatively, a longer time may be required for a sweep to happen than was represented by our sampling scheme (1 month). While this hypothesis remains to be experimentally tested, it does provide a plausible mechanism that would maintain sequence-discrete populations despite such intrapopulation gene-content diversity, frequent HGT, and environmental transitions. Consistent with this working hypothesis, we observe similar patterns of intrapopulation diversity in *Salinibacter ruber* [21], the most abundant bacterial species of the salterns, indicating that similar mechanisms may apply between the two domains of life. Moreover, these results further corroborate the use of sequence-discrete populations as the important unit of microbial diversity for taxonomy as well as for future investigations for advancing taxonomy and diversity studies.

The results presented here require further experimentation to understand whether the cyclic changes in ionic strength promote either an evolution of the dominant ecotype that may explain the differences between the initial and final gene repertoire, or whether the auxiliary pangenome gene pool dynamics among co-occurring strains would guarantee the success of the dominant ecotype on a longer temporal scale. Perhaps, the “microbial weed” behavior of

Hqr. walsbyi and *Sal. ruber* is not really due to their exceptional vigor and competitive ability [55] but to a wide range of co-existing ecotypes that carry a vast auxiliary pangenome [21] guaranteeing their preponderance in a severely fluctuating system.

Acknowledgements The authors would like to thank Arantxa López for DNA extraction and Vladimir Benes for metagenomes sequencing. The authors would especially like to thank the whole team at Salinas d'Es Trenc and Gusto Mundial Balearides, S.L. (Flor de Sal d'Es Trenc) for allowing access to their facilities and their support in performing the experiments. This study was funded by the Spanish Ministry of Economy projects CGL2012-39627-C03-03, CLG2015_66686-C3-1-P and PGC2018-096956-B-C41 (to RRM), CGL2015_66686-C3-3-P (to JA) and also supported with European Regional Development Fund (FEDER) funds. RA was financed by the Max Planck Society. KTK's research was supported, in part, by the U. S. National Science Foundation (Award No. 1831582). TV received a pre-doctoral fellowship (Nr BES-2013-064420) from the Spanish Government Ministry for Finance and Competition. RRM acknowledges the financial support of the sabbatical stay at Georgia Tech supported by the grant PRX18/00048 of the Ministry of Sciences, Innovation and Universities.

Compliance with ethical standards

Conflict of interest The authors declare that they have no conflict of interest.

Publisher's note Springer Nature remains neutral with regard to jurisdictional claims in published maps and institutional affiliations.

References

- Viver T, Orellana LH, Díaz S, Urdiain M, Ramos-Barbero MD, González-Pastor JE, et al. Predominance of deterministic microbial community dynamics in salters exposed to different light intensities. *Environ Microbiol.* 2019;21:4300–15.
- Tettelin H, Masignani V, Cieslewicz MJ, Donati C, Medini D, Ward NL, et al. Genome analysis of multiple pathogenic isolates of *Streptococcus agalactiae*: implications for the microbial "pan-genome". *Proc Natl Acad Sci USA.* 2005;102:13950–5.
- Amann R, Rosselló-Móra R. After all, only millions? *MBio.* 2016;7:e00999–16.
- Konstantinidis KT, Ramette A, Tiedje JM. The bacterial species definition in the genomic era. *Philos Trans R Soc Lond B Biol Sci.* 2006;361:1929–40.
- Shapiro BJ, Polz MF. Ordering microbial diversity into ecologically and genetically cohesive units. *Trends Microbiol.* 2014;22:235–47.
- McInerney JO, McNally A, O'Connell MJ. Why prokaryotes have pangenomes. *Nat Microbiol.* 2017;2:17040.
- Andreani NA, Hesse E, Vos M. Prokaryote genome fluidity is dependent on effective population size. *ISMEJ.* 2017;11:1719–21.
- Cohan FM. What are bacterial species? *Annu Rev Microbiol.* 2002;56:457–87.
- Lan R, Reeves PR. When does a clone deserve a name? A perspective on bacterial species based on population genetics. *Trends Microbiol.* 2001;9:419–24.
- Fraser C, Alm EJ, Polz MF, Spratt BG, Hanage WP. The bacterial species challenge: making sense of genetic and ecological diversity. *Science.* 2009;323:741–46.
- Vázquez DP, Simberloff D. Ecological specialization and susceptibility to disturbance: conjectures and refutations. *Am Nat.* 2002;159:606–23.
- Prosser JI, Bohannan BJM, Curtis TP, Ellis RJ, Firestone MK, Freckleton RP, et al. The role of ecological theory in microbial ecology. *Nat Rev Microbiol.* 2007;5:384–92.
- Shade A, Peter H, Allison SD, Baho DL, Berga M, Bürgmann H, et al. Fundamentals of microbial community resistance and resilience. *Front Microbiol.* 2012;3:417.
- Rodríguez-R LM, Overholt WA, Hagan C, Huettel M, Kostka JE, Konstantinidis KT. Microbial community successional patterns in beach sands impacted by the Deepwater Horizon oil spill. *ISME J.* 2015;9:1928–40.
- Petratits PS, Latham RE, Niesenbaum RA. The maintenance of species diversity by disturbance. *Q Rev Biol.* 1989;64:393–418.
- Narasimgarao P, Podell S, Ugalde JA, Brochier-Armanet C, Emerson JB, Brocks JJ, et al. De novo metagenomic assembly reveals abundant novel major lineage of Archaea in hypersaline microbial communities. *ISME J.* 2012;6:81–93.
- Antón J, Rosselló-Móra R, Rodríguez-Valera F, Amann R. Extremely halophilic bacteria in crystallizer ponds from solar salters. *Appl Environ Microbiol.* 2000;66:3052–57.
- Gomariz M, Martínez-García M, Santos F, Rodríguez F, Capella-Gutiérrez S, Gabaldón T, et al. From community approaches to single-cell genomics: the Discovery of ubiquitous hyperhalophilic Bacteroidetes generalists. *ISME J.* 2015;9:1–16.
- Mora-Ruiz MR, Font-Verdera F, Díaz-Gil C, Urdiain M, Rodríguez-Valdecantos G, González G, et al. Moderate halophilic bacteria colonizing the phylloplane of halophytes of the subfamily *Salicornioideae* (*Amaranthaceae*). *Syst Appl Microbiol.* 2015;38:406–16.
- Antón J, Lucio M, Peña A, Cifuentes A, Brito-Echeverría J, Moritz, F, et al. High metabolomic microdiversity within co-occurring isolates of the extremely halophilic bacterium *Salinibacter ruber*. *PLoS ONE.* 2013;8:e64701.
- Conrad EC, Viver T, Hatt JK, Rosselló-Móra R, Konstantinidis KT. Unrestricted but ecologically-important gene-content diversity within a natural sequence-discrete population as revealed by sequencing of 112 isolates. 2020. In review.
- Cuadros-Orellana S, Martín-Cuadrado AB, Legault B, D'Auria G, Zhaxybayeva O, Papke RT, et al. Genomic plasticity in prokaryotes: the case of the square haloarchaeon. *ISME J.* 2007;1:235–45.
- Konopka A, Lindemann S, Fredrickson J. Dynamics in microbial communities: unraveling mechanisms to identify principles. *ISME J.* 2015;9:1488–95.
- Millán MM, Estrela MJ, Miró J. Rainfall components: variability and spatial distribution in a Mediterranean Area (Valencia Region). *J Clim.* 2005;18:2682–705.
- Santos F, Moreno-Paz M, Meseguer I, López C, Rosselló-Móra R, Parro V, et al. Metatranscriptomic analysis of extremely halophilic viral communities. *ISME J.* 2011;5:1621–33.
- Begon M, Townsend CR, Harper JL, editors. *Ecology: from individuals to ecosystems.* 4th ed. Malden, MA, USA: Blackwell Publishing Ltd; 2006.
- Rodríguez-R LM, Konstantinidis KT. Nonpareil: a redundancy-based approach to assess the level of coverage in metagenomics datasets. *Bioinform.* 2014;30:629–35.
- Ondov BD, Treangen TJ, Melsted P, Mallonee AB, Bergman NH, Koren S, et al. Mash: fast genome and metagenome distance estimation using MinHash. *Genome Biol.* 2016;17:132.
- Oksanen J, Kindt R, Legendre P, O'Hara B. *Vegan: community ecology package.* *Com Ecol Pack.* 2007;10:631–37.
- Pruesse E, Quast C, Knittel K, Fuchs BM, Ludwig W, Peplies J, et al. SILVA: a comprehensive online resource for quality checked

- and aligned ribosomal RNA sequence data compatible with ARB. *Nucleic Acids Res.* 2007;35:7188–96.
31. Ludwig W, Strunk O, Westram R, Richter L, Meier H, Yadhukumar, et al. ARB; a software environment for sequence data. *Nucleic Acids Res.* 2004;32:1363–71.
 32. Wu YW, Tang YH, Tringe SG, Simmons BA, Singer SW. MaxBin: an automated binning method to recover individual genomes from metagenomes using an expectation-maximization algorithm. *Microbiome.* 2014;2:26.
 33. Rodríguez-R LM, Gunturu S, Harvey WT, Rosselló-Móra R, Tiedje JM, Cole JR, et al. The Microbial Genomes Atlas (MiGA) webserver: taxonomic and gene diversity analysis of *Archaea* and *Bacteria* at the whole genome level. *Nucleic Acids Res.* 2018;46:W282–8.
 34. Altschul SF, Gish W, Miller W, Myers EW, Lipman DJ. Basic local alignment search tool. *J Mol Biol.* 1990;215:403–10.
 35. Eren AM, Esen ÖC, Quince C, Vineis JH, Morrison HG, Sogin ML, et al. Anvi'o: an advanced analysis and visualization platform for 'omics data. *PeerJ.* 2015;3:e1319.
 36. Hyatt D, Chen GL, LoCascio PF, Land ML, Larimer FW, Hauser LJ. Prodigal: prokaryotic gene recognition and translation initiation site identification. *BMC Bioinform.* 2010;11:119.
 37. UniProt Consortium. Uniprot: a hub for protein information. *Nucleic Acids Res.* 2015;43:D204–12.
 38. Rodríguez-R LM, Konstantinidis KT. The enveomics collection: a toolbox for specialized analyses of microbial genomes and metagenomes. *PeerJ Prepr.* 2016;4:e1900v1.
 39. Caro-Quintero A, Konstantinidis KT. Bacterial species may exist, metagenomics reveal. *Environ Microbiol.* 2012;14:347–55.
 40. Goris J, Konstantinidis KT, Klappenbach JA, Coenye T, Vandamme P, Tiedje JM. DNA-DNA hybridization values and their relationship to whole-genome sequence similarities. *Int J Syst Evol Microbiol.* 2007;57:81–91.
 41. Viver T, Orellana LH, Hatt JK, Urdiain M, Díaz S, Richter M, et al. The low diverse gastric microbiome of the jellyfish *Cotylorhiza tuberculata* is dominated by four novel taxa. *Environ Microbiol.* 2017;19:3039–58.
 42. Haynes WM, Lide DR, Bruno TJ, editors. *CRC handbook of chemistry and physics*, 94th ed. London, UK: CRC Press; 2013. p. 4–89.
 43. Griebler C, Lueders T. Microbial biodiversity in groundwater ecosystems. *Freshw Biol.* 2009;54:649–77.
 44. Konstantinidis KT, Tiedje JM. Towards a genome-based taxonomy for prokaryotes. *J Bacteriol.* 2005;187:6258–64.
 45. Oren A. Microbial life at high salt concentrations: phylogenetic and metabolic diversity. *Saline Syst.* 2008;4:2.
 46. Pedrós-Alió C. Marine microbial diversity: can it be determined? *Trends Microbiol.* 2006;14:257–63.
 47. Azua-Bustos A, Fairén AG, González-Silva C, Ascaso C, Carrizo D, Fernández-Martínez MÁ, et al. Unprecedented rains decimate surface microbial communities in the hyperarid core of the Atacama Desert. *Sci Rep.* 2018;8:16706.
 48. Allison SD, Martiny JHB. Resistance, resilience, and redundancy in microbial communities. *Proc Natl Acad Sci U S A.* 2008;105:11512–19.
 49. Uritskiy G, Getsin S, Munn A, Gomez-Silva B, Davila A, Glass B, et al. Halophilic microbial community compositional shift after a rare rainfall in the Atacama Desert. *ISME J.* 2019;13:2737–49.
 50. Ghai R, Pašić L, Fernández AB, Martín-Cuadrado AB, Mizuno CM, McMahon KD, et al. New abundant microbial groups in aquatic hypersaline environments. *Sci Rep Nat* 2011;1:135.
 51. Burns DG, Janssen PH, Itoh T, Minegishi H, Usami R, Kamekura M, et al. *Natronomonas moolapensis* sp. nov., non-alkaliphilic isolates recovered from a solar saltern crystallizer pond, and emended description of the genus *Natronomonas*. *Int J Syst Evol Microbiol.* 2010;60:1173–76.
 52. López-Pérez M, Ghai R, Leon MJ, Rodríguez-Olmos Á, Copá-Patiño JL, Soliveri J, et al. Genomes of “*Spiribacter*”, a streamlined, successful halophilic bacterium. *BMC Genom.* 2013;14:787.
 53. Martín-Cuadrado AB, Pašić L, Rodríguez-Valera F. Diversity of the cell-wall associated genomic island of the archaeon *Haloquadratum walsbyi*. *BMC Genom.* 2015;16:603.
 54. Mirete S, Mora-Ruiz MF, Lamprecht-Grandío M, de Figueras CG, Rosselló-Móra R, González-Pastor J. Salt resistance genes revealed by functional metagenomics from brines and moderate-salinity rhizosphere within a hypersaline environment. *Front Microbiol.* 2015;6:1121.
 55. Cray JA, Bell AN, Bhaganna P, Mswaka AY, Timson DJ, Hallsworth JE. The biology of habitat dominance; can microbes behave as weeds? *Microb Biotechnol.* 2013;6:453–92.